Locomotion Behavior Is Affected by the $G\alpha_S$ Pathway and the Two-Pore-Domain K^+ Channel TWK-7 Interacting in GABAergic Motor Neurons in *Caenorhabditis elegans*

Dieter-Christian Gottschling, Frank Döring, and Kai Lüersen[1]
Department of Molecular Prevention, Institute of Human Nutrition and Food Science, Christian-Albrechts-University of Kiel, 24118, Germany

ABSTRACT Adjusting the efficiency of movement in response to environmental cues is an essential integrative characteristic of adaptive locomotion behavior across species. However, the modulatory molecules and the pathways involved are largely unknown. Recently, we demonstrated that in *Caenorhabditis elegans*, a loss-of-function of the two-pore-domain potassium (K_2P) channel TWK-7 causes a fast, coordinated, and persistent forward crawling behavior in which five central aspects of stimulated locomotion—velocity, direction, wave parameters, duration, and straightness—are affected. Here, we isolated the reduction-of-function allele *cau1* of the *C. elegans* gene *kin-2* in a forward genetic screen and showed that it phenocopies the locomotor activity and locomotion behavior of *twk-7(null)* animals. *Kin-2* encodes the negative regulatory subunit of protein kinase A (KIN-1/PKA). Consistently, we found that other gain-of-function mutants of the $G\alpha_S$-KIN-1/PKA pathway resemble *kin-2(cau1)* and *twk-7(null)* in locomotion phenotype. Using the powerful genetics of the *C. elegans* system in combination with cell type-specific approaches and detailed locomotion analyses, we identified TWK-7 as a putative downstream target of the $G\alpha_S$-KIN-1/PKA pathway at the level of the γ-aminobutyric acid (GABA)ergic D-type motor neurons. Due to this epistatic interaction, we suggest that KIN-1/PKA and TWK-7 may share a common pathway that is probably involved in the modulation of both locomotor activity and locomotion behavior during forward crawling.

KEYWORDS *C. elegans*; PKA; locomotion; motor neurons; two-pore-domain potassium channel

LOCOMOTION is crucial for almost all aspects of animal behavior including escape, foraging, and mating. From invertebrates to limbed vertebrates, the rhythmic output of motor neurons promotes coordinated, repetitive contractions of antagonistic muscles to generate coherent gaits such as crawling, walking, swimming, or running. Usually, these rhythmic motor activities are controlled by neural circuits called central pattern generator networks (Marder *et al.* 2005; Grillner 2006; Kiehn 2006), which have intrinsic rhythmic outputs. It is well-documented that oscillatory networks are affected by neuromodulators and modulatory neurons, leading to altered frequencies, phase relationships, and functional interactions among neurons (Bargmann 2012; Marder *et al.* 2014). Such reconfigurations of neuronal output are prerequisites for adaptive motor behavior and enable organisms to respond to varying external and internal cues. Adapting movement in response to temperature, food availability, nutritional state, or tactile stimulation is an example of such adjustment. However, the modulatory molecules, pathways, and targets that are involved are largely unknown.

A number of studies have reported that the nematode *Caenorhabditis elegans* exhibits adaptation of its locomotor activity and locomotion behavior in response to changing environmental conditions and internal physiological states such as land/water transition, partial pressure of oxygen, viscosity, mechanical stimulation, temperature, food availability, and starvation or dietary restriction (Sawin *et al.* 2000; Gaglia and Kenyon 2009; Vidal-Gadea *et al.* 2011; Edwards *et al.* 2012; Ma *et al.* 2013; Lüersen *et al.* 2014).

Copyright © 2017 by the Genetics Society of America
doi: https://doi.org/10.1534/genetics.116.195669
Manuscript received September 8, 2016; accepted for publication March 19, 2017; published Early Online March 24, 2017.
Supplemental material is available online at www.genetics.org/lookup/suppl/doi:10.1534/genetics.116.195669/-/DC1.
[1]Corresponding author: Department of Molecular Prevention, Institute of Human Nutrition and Food Science, Christian-Albrechts-University of Kiel, Heinrich-Hecht-Platz 10, 24118 Kiel, Germany. E-mail: luersen@foodsci.uni.kiel.de

C. elegans crawls with dorsoventral sinusoidal waves on solid substrates or swims with C-shaped thrashes in liquids (Gray and Lissmann 1964; Vidal-Gadea *et al.* 2011). Undulatory locomotion is driven by three classes of motor neurons present in the ventral nerve cord of the worm. The excitatory cholinergic A- and B-type motor neurons, which are further divided into ventral (V) and dorsal (D) subclasses, innervate longitudinally aligned ventral and dorsal muscle cells (White *et al.* 1976; Wen *et al.* 2012; Gjorgjieva *et al.* 2014), thereby promoting backward and forward locomotion, respectively (Chalfie *et al.* 1985). Wen *et al.* (2012) showed that the B-type motor neurons responsible for forward locomotion are coupled to proprioception. Hence, rhythmic bending is suggested to be driven along the body by a chain of reflexes. The third class of motor neurons, the inhibitory D-type motor neurons (VD and DD), are postsynaptic to the cholinergic A- and B-type motor neurons of the opposite side, leading to contralateral muscle inhibition (White *et al.* 1976; Wen *et al.* 2012; Gjorgjieva *et al.* 2014). Ablation of D-type motor neurons results in worms that respond to head touch with body shrinkage instead of the backward escape movement. Remarkably, spontaneous forward locomotion is not prevented (McIntire *et al.* 1993). However, modulation of D-type motor neuron function has been demonstrated to significantly alter wave parameters and to impair coordinated crawling (Donnelly *et al.* 2013; Lüersen *et al.* 2016).

In *C. elegans*, neurotransmitter release from synaptic vesicles of motor neurons is regulated by a network of three canonical heterotrimeric G protein signaling pathways, namely, $G\alpha_q$, $G\alpha_0$ and $G\alpha_S$. The diacylglycerol (DAG)-producing $G\alpha_q$ pathway represents the core pathway that promotes the release of acetylcholine, the major excitatory neurotransmitter at neuromuscular junctions. The $G\alpha_q$ homolog EGL-30 exerts its stimulating function in acetylcholine release through EGL-8/PLCβ and PLC-3/PLCγ, two parallel-acting phospholipase C proteins (Yu *et al.* 2013). DAG levels and hence acetylcholine release are negatively regulated by DAG kinase DGK-1 and the $G\alpha_o$ pathway through GOA-1/G protein α subunit G_o. Accordingly, gain-of-function mutants of *egl-30* or loss-of-function mutants of *goa-1* and *dgk-1* were found to move hyperactively on agar plates (Nurrish *et al.* 1999). $G\alpha_q$ loss-of-function mutants are lethargic or move slowly (Lackner *et al.* 1999; Miller *et al.* 1999; Reynolds *et al.* 2005). In addition, the $G\alpha_S$ signaling pathway has been reported to control *C. elegans* crawling activity by interaction with the $G\alpha_q$ pathway; however, it is downstream of DAG production. Gain-of-function mutants with overactivation of cAMP-dependent protein kinase A (PKA/KIN-1) are hyperactive (Reynolds *et al.* 2005; Schade *et al.* 2005). The downstream targets of PKA/KIN-1 involved in this process have not yet been identified (Reynolds *et al.* 2005; Zhou *et al.* 2007).

Recently, we found that the two-pore-domain potassium (K_2P) channel TWK-7 is required in motor neurons to maintain the normal spontaneous locomotion behavior of *C. elegans* (Lüersen *et al.* 2016). Inactivation of TWK-7 in B-type motor neurons led to accelerated but still coordinated spontaneous crawling with slightly flattened amplitudes, whereas *twk-7(null)* worms rescued by overexpressing *twk-7* specifically in B-type or D-type motor neurons exhibited slower and less directed spontaneous locomotion with altered amplitudes and wavelengths. Moreover, the abundance of TWK-7 also affected the swimming activity of *C. elegans*. The *twk-7(null)* mutants were characterized by enhanced, and rescue animals by reduced, body-bending swimming activity. K_2P channels are regulatory background leak channels that play an essential role in setting the resting membrane potential. Hence, they determine the excitability of many cell types including motor neurons. Consequently, K_2P channels are putative modulators of muscle activity (Perrier *et al.* 2003; Larkman and Perkins 2005; Enyedi and Czirjak 2010). The activity of K_2P channels can be modulated by a variety of factors including pH, temperature, membrane stretch, G protein-coupled receptor pathways, polyunsaturated fatty acids, and medicinal agents such as volatile anesthetics (Gray *et al.* 2000; Yost 2000; Patel and Honore 2001; Aryal *et al.* 2015; Zhang *et al.* 2015). Accordingly, we suggested that TWK-7 may be involved in the regulation of locomotor activity and behavior of *C. elegans* (Lüersen *et al.* 2016).

In the present study, we have performed a forward genetic screen to identify putative regulators of *C. elegans* TWK-7 channel function. To this end, we identified mutants that showed enhanced and coordinated body-bending swimming frequencies comparable to *twk-7(null)* mutants. We isolated the allele *cau1* of the gene *kin-2*, encoding the negative regulatory subunit of PKA/KIN-1. In agreement with a previous study on a *kin-2* reduction-of-function allele (Schade *et al.* 2005), our *kin-2(cau1)* worms also exhibit enhanced crawling activity. Detailed, in-depth comparative locomotion analyses revealed that *kin-2(cau1)* and other $G\alpha_S$ gain-of-function *(gf)* mutants phenocopy *twk-7(null)* animals to a great extent. Genetic interaction studies in combination with cell type-specific expression approaches indicate that the $G\alpha_S$ -KIN-1/PKA pathway may be an upstream regulator of TWK-7.

Materials and Methods

Strains and culturing

All *C. elegans* strains were grown at 20° on nematode growth media (NGM) agar plates seeded with *Escherichia coli* OP50 as a food source (Brenner 1974). *C. elegans kin-2(cau1)* was isolated in an F2 genetic screen for worms that exhibit enhanced body-bending swimming frequency (BBSF) following a standard ethyl methanesulfonate mutagenesis protocol (Jorgensen and Mango 2002). The *cau1* mutant allele responsible for the locomotion phenotype was identified by SNP mapping using the wild-type strain CB4856 in combination with whole-genome sequencing (Minevich *et al.* 2012). The following strains were obtained from the *Caenorhabditis* Genetics Center: Bristol N2 (used as wild-type), *egl-30(ad805)I*,

goa-1(n1134)I, *gsa-1(ce94)I*, *unc-29(e403)I*, *pde-4(ce268)II*, *twk-7(nf120)III*, *egl-8(e2917)V*, *dgk-1(nu62)X*, and *kin-2(c179)X*. Double mutants were generated by crossing using standard genetic methods without additional marker mutations. Homozygosity of alleles in each double mutant was confirmed by PCR in case of deletion mutations, by restriction length polymorphism analysis in case of appropriate SNP mutations or, in all other cases, by sequencing of amplified genomic DNA.

Molecular biology and transfection of C. elegans

The D-type neuron-specific dominant negative *kin-2* construct *unc-47p*::*KIN-2(G^{310}D)* and the rescue construct *unc-47p*::*KIN-2* were kindly provided by Derek Sieburth (University of Southern California) (Wang and Sieburth 2013). For B-type neuron-specific rescue, we exchanged the *unc-47p* fragment for 4.12 kb of the *acr-5* promoter region, leading to an *acr-5p*::*KIN-2* construct. The transgenic *acr-5p*::*TWK-7*::*mCherry*::*let-858(3′UTR)* and *unc-47p*::*TWK-7*::*mCherry*::*let-858(3′UTR)* have been previously generated (Lüersen *et al.* 2016). The transgenic strains were generated by biolistic bombardment following the protocol of Wilm *et al.* (1999). For rescue experiments, the *myo-2p*::GFP::pPD118.33 plasmid was used as a comarker.

Locomotion assays and analyses

The swimming activity of young adult *C. elegans* (age 72 hr) was analyzed as previously described (Lüersen *et al.* 2014). Briefly, worms in a 50 μl droplet of M9 buffer were placed on a diagnostic slide (three wells, 10 mm diameter; Menzel) and immediately filmed for 1 min with a VRmagic C-9+/BW PRO IR-CUT camera (VRmagic, Germany) attached to a Zeiss Stemi 2000-C microscope (Zeiss [Carl Zeiss], Thornwood, CA). The resulting MOV files were used to quantify the BBSF using the ImageJ wrMTrck worm tracker plugin according to the protocol described in http://www.phage.dk/plugins/download/wrMTrck.pdf. One body bend corresponds to the movement of the head region thrashing from one side to the other and back to the starting position.

Locomotion analyses on NGM agar plates were carried out as described in Lüersen *et al.* (2016). The assay was set up by placing 500 late L3- or early L4-stage larvae on locomotion assay plates spread with a thin lawn of OP50 bacteria (100 μl of an OP50 overnight culture per plate, incubated for 20 hr at 37°). After incubation at 20° for 24 hr, the locomotion of at least five young adult animals was captured as MOV files three times for 1 min each on different plate regions with a VRmagic C-9+/BW PRO IR-CUT camera (VRmagic) attached to a Zeiss Stemi 2000-C microscope (Zeiss). Crawling velocity and straightness rates were quantified using the ImageJ wrMTrck worm tracker plugin. Spontaneous body-bending crawling frequency (BBCF) was counted visually frame-by-frame for worms that were captured for at least 5 sec by the camera. One body bend corresponds to the movement of the tip of the tail from one side to the other. The straightness rate was calculated from the ratio of traveled distance to track length, in which the traveled distance represents the straight line from the start-to-end coordinates of each recorded animal. In addition, a more detailed analysis split locomotion behavior into forward, backward, and dwelling time periods. The latter includes periods when the worms move less than one body bend forward or backward. Furthermore, we determined the relative time the worms spent on dwelling and forward and backward locomotion.

Stimulated forward locomotion assays were conducted as described in Gaglia and Kenyon (2009). Staged young adult animals were transferred with a worm pick from standard NGM plates to NGM assay plates spread with a thin lawn of OP50 food bacteria (100 μl of an overnight culture at 37°). Videos were taken immediately after transfer and every 30 min for 2 hr to measure the persistence of locomotor activity. BBCF was assessed visually frame-by-frame from the recorded movies. Velocities and straightness rates were analyzed using the ImageJ wrMTrck worm tracker plugin.

Measurement of wave parameters

Wave parameters were determined using recorded movies processed with ImageJ software. The calibration was adjusted for a resolution of 640 × 480 pixels at 64 pixels/mm. Worm lengths, wave lengths, and amplitudes of sinusoidal undulation were measured using the scaled fragmented line tool along the body axes of at least three worms from each video for a period of five body bends per worm.

Pharmacological assays

Aldicarb and levamisole sensitivity assays were performed as blind experiments (Schade *et al.* 2005; Mahoney *et al.* 2006). Briefly, 25–30 synchronized young adult worms (age: 3 days) were transferred to the center of a 60 mm NGM plate (spot 5 μl bacteria) containing 1 mM aldicarb or 0.5 mM levamisole, and the percentage of paralyzed animals was monitored over time. Locomotion was assessed by prodding animals with a platinum wire every 15 min following exposure to the drug. Worms that failed to respond to this stimulus were classified as paralyzed.

Data availability

The authors state that all data necessary for confirming the conclusions presented in the article are represented fully within the article. All strains and reagents used in this work will be made available upon request.

Results

Isolation of a novel kin-2(cau1) allele that enhances locomotor activity

In a genetic screen for *C. elegans* worms with an enhanced and coordinated BBSF, we isolated the *kin-2* allele *cau1*. Compared to wild-type animals with a bending rate of 1.71 ± 0.1 Hz, the rate in *cau1* worms was increased by 0.52 Hz (Figure 1A). The *kin-2(cau1)* mutant strain also crawled on agar plates with an elevated spontaneous body-bending rate

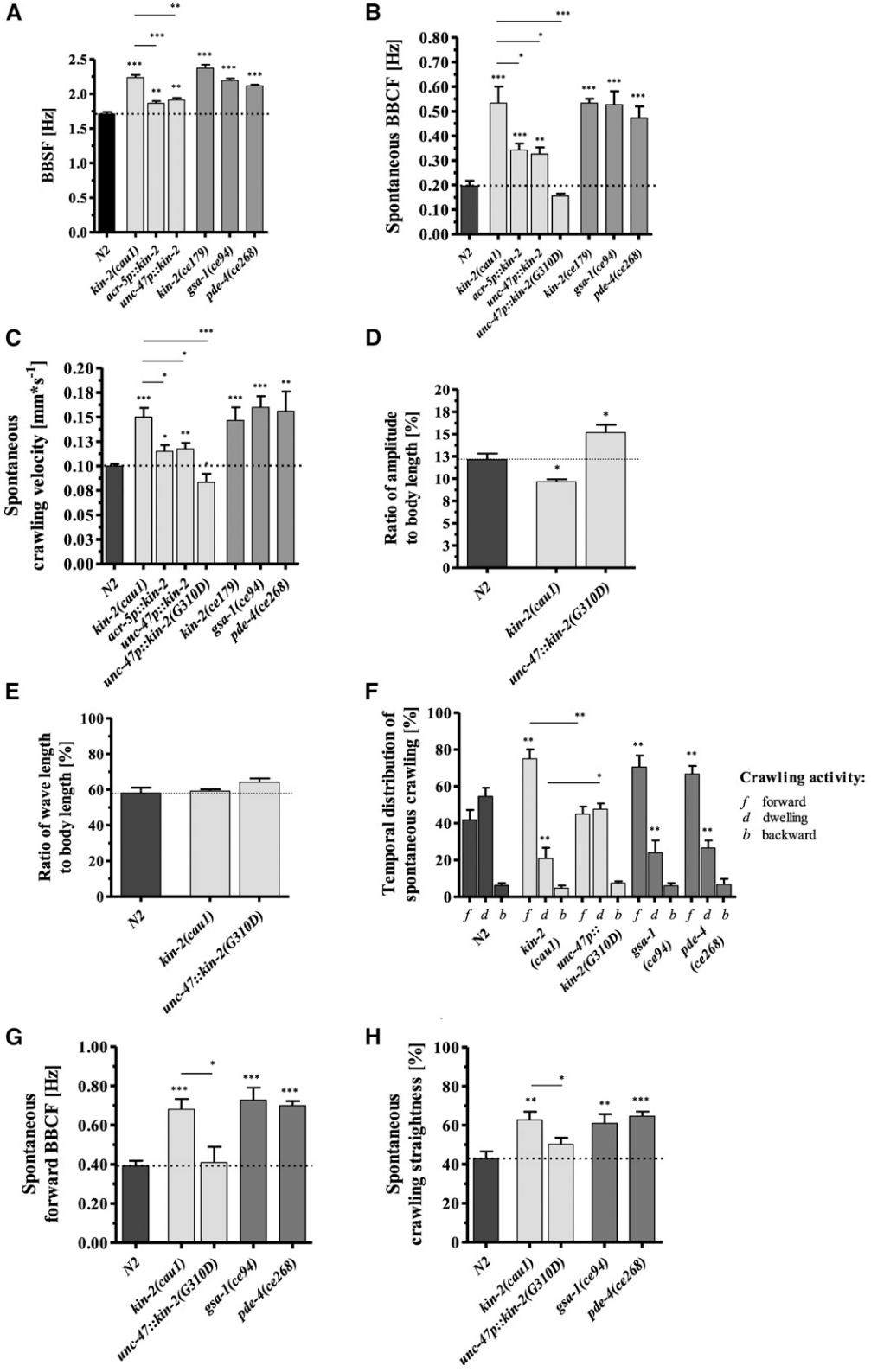

Figure 1 *kin-2(cau1)*, a mutant allele of the regulatory subunit of KIN-1/PKA, produces increased spontaneous locomotor activity and locomotion behavior similar to the phenotype of $G\alpha_S$*(gf)* mutants. (A) *kin-2(cau1)* and $G\alpha_s$*(gf)* mutants exhibit elevated BBSF. Enhanced swimming activity of *kin-2(cau1)* worms is rescued by overexpression of wild-type KIN-2 in cholinergic B-type and GABAergic D-type motor neurons. (B) *kin-2(cau1)* and $G\alpha_S$*(gf)* mutants crawl with enhanced spontaneous BBCF and (C) increased velocities. The elevated crawling activity is rescued by overexpression of wild-type KIN-2 in cholinergic B-type and GABAergic D-type motor neurons, or by overexpression of dominant negative KIN-2($G^{310}D$) in GABAergic neurons. (D) Compared with wild-type worms, the ratios of amplitude to body length of *kin-2(cau1)* mutants during spontaneous crawling are significantly lower. In

(0.20 ± 0.05 Hz *vs.* 0.53 ± 0.15 Hz) (Figure 1B), resulting in an increased average crawling speed of 0.15 ± 0.02 mm*s^{-1} compared with the spontaneous velocity of wild-type worms (0.10 ± 0.01 mm*s^{-1}) (Figure 1C).

KIN-2/RIβ represents the cAMP-dependent regulatory subunit of KIN-1/PKA. The *cau1* allele carries a G-to-A transition at nt 275 of the coding region, resulting in an R^{92}H substitution in the polypeptide sequence (Supplemental Material, Figure S1A in File S8). The R^{92} is part of the pseudosubstrate site of the inhibitory domain of KIN-2/RIβ (Schade *et al.* 2005). A similar R^{92}C exchange within this small pseudosubstrate domain has been previously identified in the strong reduction-of-function *kin-2* allele *ce179* (Figure S1A in File S8) (Schade *et al.* 2005). In good accordance with that finding, *kin-2(ce179)* was characterized as hyperactive on plates. Our data revealed that the *kin-2(ce179)* allele with an R^{92}C and the *kin-2(cau1)* allele with an R^{92}H exchange exhibited similar increased swimming and crawling activity (Figure 1, A–C). The evolutionarily conserved Arg^{92} residue is suggested to be crucial for the inhibitory effect of KIN-2/RIβ. Its mutation causes an enhanced sensitivity of the KIN-1/KIN-2 (PKA/RIβ) holoenzyme to the activator cAMP (Schade 2005). In *C. elegans*, KIN-1/PKA is widely expressed in the nervous system including the motor neurons of the ventral nerve cord (McKay *et al.* 2003; WormBase). As shown in Figure 1, A–C, overexpression of wild-type KIN-2 in B-type or D-type motor neurons of *cau1* worms was sufficient to rescue both locomotion phenotypes. We suggest that the reduced sensitivity of wild-type KIN-2/RIβ to cAMP reduced KIN-1/PKA signaling in the motor neurons of transgenic *cau1* worms.

We next asked whether the inactivation of KIN-1/PKA specifically in cholinergic B-type or γ-aminobutyric acid (GABA)ergic motor neurons would have a similar or even more drastic rescue effect. To this end, we employed the dominant negative *kin-2(G^{310}D)* construct generated by Wang and Sieburth (2013). Due to the G^{310}D exchange, the mutated KIN-2/RIβ is insensitive to cAMP. Hence, it inhibits the KIN-1/PKA pathway by preventing the dissociation of the KIN-1/PKA holoenzyme. Unfortunately, in the *kin-2(cau1)* genetic background, overexpression of dominant negative KIN-2(G^{310}D) in B-type neurons under the *acr-5* promoter was lethal. In contrast, worms transfected with the GABAergic neuron-specific *unc-47*p::*kin-2(G^{310}D)* construct produced viable progeny. Notably, this construct rescued the elevated locomotor activity of *kin-2(cau1)* mutants (Figure 1, B and C). Taken together, the results show that alterations in the activity of the KIN-1/PKA pathway in B-type and D-type motor neurons affect the locomotor activity of *C. elegans*.

kin-2(cau1) mutants show altered body shape and locomotion behavior during spontaneous crawling

kin-2(cau1) mutant worms are smaller (Figure S2A in File S8) and consequently moved with significantly reduced amplitudes (Figure S2B in File S8) and wavelengths (Figure S2C in File S8) during spontaneous forward crawling compared with wild-type animals (absolute values). To compare wave shape parameters in animals of different lengths, we calculated the amplitudes and wavelengths in terms of body lengths and found a reduced amplitude-to-body-length ratio for the *kin-2(cau1)* mutants (9.67 ± 0.38% of body length) compared to wild-type worms (12.15 ± 0.96% of body length) (Figure 1D). The ratios of wavelengths to body lengths revealed no significant differences among the tested strains (Figure 1E). Rescue of *kin-2(cau1)* by dominant negative *kin-2*(G^{310}D) in GABAergic neurons led to elevated amplitude-to-body-length ratios during spontaneous crawling (Figure 1, D and E). Interestingly, stimulation of forward crawling by picking transfer increased the amplitude-to-body-length ratios of these transgenic worms even further. In contrast, stimulated wild-type animals reduced the corresponding amplitude-to-body-length ratios to the level of the *kin-2(cau1)* mutants (File S1, File S2, and File S3).

Next, a detailed analysis of spontaneous crawling behavior revealed that *kin-2(cau1)* mutants spent ∼35% more time crawling forward with enhanced locomotor activity at the expense of dwelling periods (Figure 1, F and G) and exhibited ∼20% increased straightness rates in comparison with wild-type worms (Figure 1H). When analyzing the spontaneous crawling behavior of *kin-2(cau1)* transgenic animals expressing the dominant negative *kin-2(G^{310}D)* allele in GABAergic motor neurons, we found that the persistent straightforward locomotion exhibited by *kin-2(cau1)* mutant animals became drastically altered. The time spent crawling forward was reduced by almost 50% in transgenic worms (Figure 1F) and their straightness values dropped from ∼80 to 50% (Figure 1, G and H).

Taken together, compared to wild-type worms, *kin-2(cau1)* mutants show enhanced locomotor activities, conspicuous

contrast, transgenic worms overexpressing dominant negative KIN-2(G^{310}D) exhibit increased amplitudes during spontaneous crawling. (E) The ratios of wavelength to body length of *kin-2(cau1)* mutants and transgenics during spontaneous crawling are similar and wild-type-like. (F) During spontaneous movement, *kin-2(cau1)* and Gα_s*(gf)* animals spend more time crawling forward and less time dwelling: f, forward; b, backward; d, dwelling. Overexpression of dominant negative KIN-2(G^{310}D) rescues the hyperactive Gα_s*(gf)* phenotype to the wild-type level. (G) *kin-2(cau1)* and Gα_s*(gf)* alleles induce elevated BBCF during spontaneous forward crawling (in contrast to (B), periods of dwelling and backward crawling are not considered here), whereas transgenic worms overexpressing dominant negative KIN-2(G^{310}D) show wild-type-like body-bending activity. (H) The crawling behavior of *kin-2(cau1)* and Gα_S*(gf)* animals is characterized by markedly enhanced straightness rates compared to that of the corresponding transgenic and wild-type animals. All values in (A–C) and (F–H) represent the mean (± SEM) of $N \geq 3$ independent experiments involving $n \geq 30$ never-starved animals. For the measurement of wave parameters in (D) and (E), $N = 3$ independent experiments with $n = 15$ worms per trial were evaluated. *$P < 0.05$, **$P < 0.01$, and ***$P < 0.001$ (Student's *t*-test). Dotted lines indicate the wild-type level. BBCF, body-bending crawling frequency; BBSF, body-bending swimming frequency; GABA, γ-aminobutyric acid.

body shape modulations, and altered locomotion behaviors during spontaneous crawling.

Gα$_S$(gf) mutants show similar locomotor activity and locomotion behavior to kin-2(cau1) during spontaneous crawling

Catalytic KIN-1/PKA and regulatory KIN-2/RIβ are part of the Gα$_S$ signaling pathway. A reduction of KIN-2/RIβ activity causes a gain-of-function of Gα$_S$ signaling because it is a negative regulator of KIN-1/PKA. Hence, we next tested the corresponding upstream G protein GSA-1 and the phosphodiesterase PDE-4, a negative regulator of Gα$_S$ signaling, for their effects on locomotor activity. Consistent with previous reports (Charlie *et al.* 2006; Hu *et al.* 2011), the two Gα$_S$*(gf)* mutant alleles *gsa-1(ce94)* and *pde-4(ce268)* also showed enhanced swimming and spontaneous crawling activity similar to that of *kin-2(cau1)* and *kin-2(ce179)* (Figure 1, A–C).

The detailed analysis of spontaneous crawling behavior revealed that Gα$_S$*(gf)* mutants allocate their time to crawling and dwelling periods in a similar manner to *kin-2(cau1)* worms (Figure 1F). Moreover, they exhibited enhanced forward locomotor activity and an ∼20% increase in straightness rates in comparison with wild-type worms (Figure 1, G and H).

Taken together, these results show that mutants with an activated Gα$_S$ pathway, compared to *kin-2(cau1)*, show similarly enhanced locomotor activity and locomotion behavior during spontaneous crawling.

Gα$_S$(gf) mutants phenocopy the spontaneous locomotor activity and locomotion behavior of twk-7(null) mutants

The locomotor activity and locomotion behavior of all Gα$_S$*(gf)* mutants were remarkably similar to those of the recently characterized *C. elegans* mutants that lack the K_2P channel TWK-7 (Lüersen *et al.* 2016). The BBCF, crawling velocities, and fast, straightforward spontaneous locomotion behavior of Gα$_S$*(gf)* mutants were essentially indistinguishable from those of *twk-7(null)* worms (Figure 2, A–E). Moreover, although *twk-7(null)* worms were the same size as wild-type worms (Figure S2A in File S8), their wave amplitude during spontaneous crawling was reduced (absolute values) (Figure S2, B and C in File S8), and therefore their ratio of amplitude to body length (9.63 ± 0.55% of body length) was similar to that of *kin-2(cau1)* mutants (see above).

Taken together, these results show that mutants with an activated Gα$_S$ pathway and *twk-7(null)* mutants resemble each other in their locomotor activity, body shape modulations, and locomotion behaviors during spontaneous crawling. Compared to wild-type worms, four different motor outputs—velocity/frequency, amplitude, direction, and persistence—are altered.

Hyperactive Gα$_{q/0}$ mutants differ from hyperactive Gα$_S$(gf) and twk-7(null) worms in their locomotion behavior during spontaneous crawling

Previous studies reported that *C. elegans* Gα$_q$ and Gα$_0$ mutants with elevated DAG and acetylcholine levels have a hyperactive phenotype (Miller *et al.* 1999; Schade *et al.* 2005). However, although these animals crawled with an enhanced body-bending frequency similar to those of Gα$_S$*(gf)* and *twk-7(null)* mutants (Figure 2, A and B), our more detailed analyses revealed a very distinct locomotion phenotype. Compared to wild-type animals, *goa-1(e1134)* and *dgk-1(nu62)* mutants did not exhibit elevated swimming activity (Figure 2C). Moreover, during spontaneous crawling, these mutants spent significantly less time crawling forward and more time dwelling and moving backward (Figure 2D), and they exhibited lower straightness rates (Figure 2E) than wild-type and Gα$_S$*(gf)* and *twk-7(null)* mutant worms.

The Gα$_S$(gf) and twk-7(null) mutants show wild-type-like responses in synaptic transmission assays

To test whether the elevated body-bending rates of *twk-7(null)* and Gα$_S$*(gf)* animals are caused by an alteration in the neuromuscular synaptic transmission of the major excitatory neurotransmitter acetylcholine, we employed a sensitivity assay with the choline esterase inhibitor aldicarb (Mahoney *et al.* 2006). Accumulation of acetylcholine in the synaptic cleft due to inhibition of its hydrolysis results in overactivation of postsynaptic cholinergic receptors and paralysis of worms. Consistent with previous studies, the control mutant alleles *dgk-1(nu62)* and *egl-8(e2917)*, representing the (*gf*) and (*lf*) alleles of the Gα$_q$ pathway, respectively, were found to be hypersensitive and resistant, respectively, to the paralytic effect of aldicarb (Figure 2F). These findings indicate an enhanced and decreased steady-state acetylcholine concentration, respectively. Remarkably, the enhanced locomotor activity of *kin-2(cau1)* worms was associated with only a slightly increased sensitivity to the choline esterase inhibitor; however, a significant difference ($P = 0.038$) was found only at time point 90 min. The time course of aldicarb-induced paralysis was unchanged in the hyperactive allele *twk-7(nf120)* compared with wild-type worms (Figure 2F).

To examine postsynaptic processes, sensitivity assays using the acetylcholine agonist levamisole were performed. Levamisole activates nicotinic acetylcholine receptors in the body-wall muscles, which causes paralysis (Fleming *et al.* 1997). In accordance with previous studies, the control allele *unc-29(e403)*, encoding a defective postsynaptic acetylcholine receptor subunit, produced a resistant phenotype (Figure 2G). Compared to the wild-type, both Gα$_S$ pathway (*gf*) mutant alleles *kin-2(cau1)* and *gsa-1(ce94)* produced a slightly, but at no time point significantly, increased sensitivity to levamisole. The time course of levamisole-induced paralysis was unchanged in *twk-7(null)* (Figure 2G).

Taken together, our results show that the *twk-7(nf120)*, *kin-2(cau1)*, and *gsa-1(ce94)* mutant worms, although hyperactive in swimming and crawling assays, did not show pronounced phenotypes in these pharmacological synaptic transmission assays. This striking discrepancy between their hyperactive locomotion phenotype and their wild-type-like sensitivity to aldicarb and levamisole suggests that, in contrast to the Gα$_q$ and Gα$_0$ pathways, TWK-7 and Gα$_S$ may affect locomotor activity without altering the levels

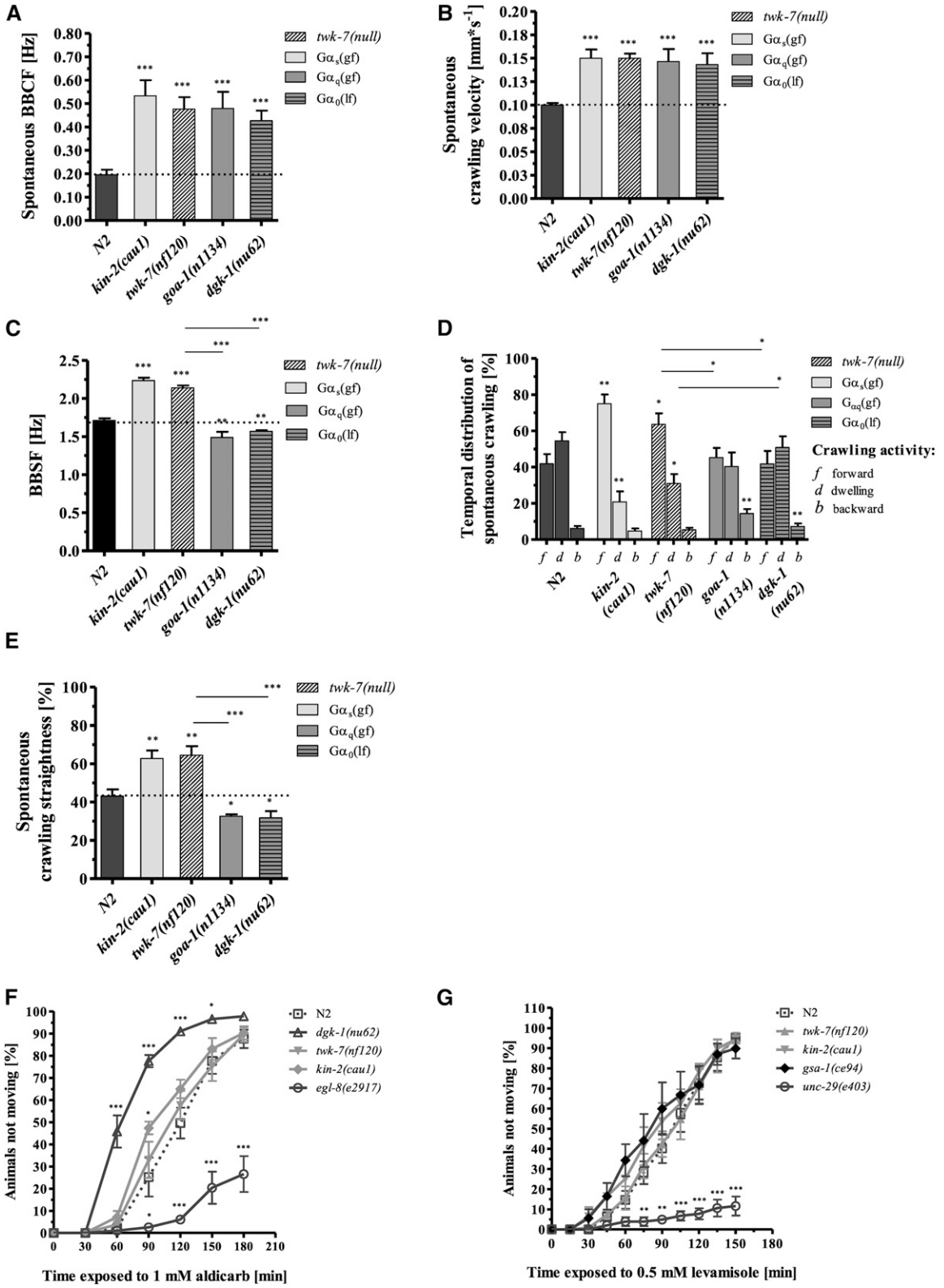

Figure 2 The elevated locomotor activity and locomotion behavior of *kin-2(cau1)* are similar to those of *twk-7(null)* but distinct from the hyperactive phenotype of $G\alpha_{q/0}$ mutant worms. (A) The hyperactive $G\alpha_{q/0}$ mutants *goa-1(n1134)* and *dgk-1(nu62)* exhibited similarly increased body-bending crawling frequencies (BBCF), (B) increased crawling velocities, and (C) decreased levels of body-bending swimming frequency (BBSF) compared with the *kin-2(cau1)* and *twk-7(null)* animals. The swimming frequencies of $G\alpha_{q/0}$ mutants were even lower than those of wild-type animals. (D) The spontaneous locomotion behavior of hyperactive $G\alpha_{q/0}$ animals is characterized by extended dwelling periods, increased backward movements, and (E) lower straightness rates compared with that of *kin-2(cau1)* and *twk-7(null)* animals. f, forward; b, backward; d, dwelling. All values represent the mean

of steady-state acetylcholine release. However, one has to keep in mind that there are some mutants in which, for unknown reasons, changes of locomotion behavior and aldicarb sensitivity do not always reflect a change in acetylcholine release (Sieburth *et al.* 2007).

Like the Gαs-KIN-1/PKA pathway, TWK-7 requires the canonical Gαq pathway for its modulatory function

It has been previously shown that the stimulating effect of activated $G\alpha_S$-KIN-1/PKA on the locomotion of *C. elegans* is strongly dependent on the canonical $G\alpha_q$ pathway (Reynolds *et al.* 2005). $G\alpha_q$ influences the crawling activity of *C. elegans* by altering the intracellular concentration of the second-messenger DAG and, hence, the acetylcholine priming and release process (Lackner *et al.* 1999; Miller *et al.* 1999; Nurrish *et al.* 1999; Reynolds *et al.* 2005). To test whether the hyperactivity-related *twk-7(null)* mutation is able to affect the lethargic phenotype of the strong $G\alpha_q$ reduction-of-function allele *egl-30(ad805)*, a double mutant was generated. The *twk-7(null)* allele was not able to substantially affect the declined locomotor activity (Figure 3, A and B) or the increased dwelling periods (Figure 3C) of the $G\alpha_q$*(lf)* mutant allele *egl-30(ad805)*. The simplest explanation for these results is that *egl-30* is *per se* required for *C. elegans* locomotion. Therefore, the stimulatory impact of inactive TWK-7 on *C. elegans* locomotion completely depends on a functional $G\alpha_q$ pathway. Similar data have been reported for activated $G\alpha_s$-KIN-1/PKA (Reynolds *et al.* 2005).

The hyperactivity-related twk-7(null) allele does not affect the locomotor activity or locomotion behavior of hyperactive Gαs-KIN-1/PKA(gf) mutants during spontaneous crawling

The high degree of similarity between the spontaneous locomotion parameters of $G\alpha_S$*(gf)* and *twk-7(null)* mutants prompted us to examine whether the $G\alpha_S$ pathway interacts genetically with *twk-7*. We generated *twk-7(null)*,*kin-2(cau1)* and *twk-7(null)*,*gsa-1(ce94)* double mutants. The *twk-7(null)* allele did not further increase spontaneous bending frequencies (Figure 4A) or velocities (Figure 4B) in a $G\alpha_S$*(gf)* genetic background compared to the respective single mutants.

The body sizes of *twk-7(null)*,*kin-2(cau1)* double mutants were as small as those of the *kin-2(cau1)* single mutants (Figure S2A in File S8), leading to similar amplitude (Figure S2B in File S8) and wavelength values (Figure S2C in File S8). Accordingly, the double mutants exhibited comparable amplitude-to-body-length ratios to those calculated for the respective single mutants, *kin-2(cau1)* and *twk-7(null)* (Figure 4C). The wavelength-to-body-length ratios were not affected in the double mutants (Figure S2, A and C in File S8). Thus, the wave shape parameters of *kin-2(cau1)* mutants were not further influenced by the introduction of the *twk-7(null)* allele.

We next found that the $G\alpha_s$*(gf)*,*twk-7(null)* double mutants and the respective single mutants spent similar amounts of time on rapid forward crawling and on dwelling during spontaneous behavior (Figure 4F). Moreover, the values of spontaneous straightness were not further increased in the $G\alpha_S$*(gf)*,*twk-7(null)* double mutants (Figure 4G). Consequently, the locomotion behavior of $G\alpha_S$*(gf)* mutants was not affected by the introduction of the *twk-7(null)* allele.

In summary, the enhanced locomotor activity and locomotion behavior during spontaneous crawling caused by an activated $G\alpha_S$ pathway were not further affected by inactive TWK-7. Thus, we suggested that the canonical $G\alpha_S$ pathway and *twk-7* might share the same genetic pathway.

Overexpression of TWK-7 in cholinergic or GABAergic motor neurons rescues the hyperactive kin-2(cau1) phenotype

To further investigate the interaction between the $G\alpha_s$ pathway and TWK-7 in *C. elegans* locomotion, we chose several cell-specific expression approaches. TWK-7 has been recently shown to be expressed in A-, B-, AS-, and D-type motor neurons of the ventral nerve cord and some unidentified head and tail neurons (Lüersen *et al.* 2016). In the same study, we demonstrated that overexpression of functional TWK-7 solely in cholinergic or GABAergic motor neurons of *twk-7(null)* animals is sufficient to cause drastically reduced spontaneous locomotor activity. Similar effects were found in the present study when TWK-7 was overexpressed in cholinergic or GABAergic motor neurons of *kin-2(cau1)* and other $G\alpha_s$ (*gf*) mutants (Figure 4, A, B, H, and I).

Moreover, *twk-7(null)* worms overexpressing TWK-7 in GABAergic motor neurons were characterized by markedly increased amplitude-to-body-length ratios (Figure 4C); the wave amplitudes were found to be further increased when forward crawling was stimulated by the picking transfer assay (Figure 4, D and E, File S4, and File S5). The same effects of TWK-7 overexpression in GABAergic neurons on spontaneous and stimulated locomotion were observed not only in wild-type worms but also in the single mutants *kin-2(cau1)* and *twk-7(null)* and in a *twk-7(null)*,*kin-2(cau1)* double mutant background (Figure 4, A–E, File S6, and File S7). When analyzing the spontaneous crawling behavior, we found that the persistent straightforward locomotion exhibited by *twk-7(null)* and *kin-2(cau1)* single mutant animals became drastically altered when TWK-7 was specifically overexpressed in GABAergic motor neurons. The time spent crawling forward

(± SEM) of at least $N \geq 3$ independent experiments involving $n \geq 30$ never-starved animals. *$P < 0.05$, **$P < 0.01$, and ***$P < 0.001$ (Student's *t*-test). Dotted lines indicate the wild-type level. (F) Aldicarb and (G) levamisole sensitivity assays. The percentage of animals that became paralyzed by each drug was monitored over time. All values represent the mean (± SEM) of at least $N \geq 3$ independent experiments involving $n \geq 75$ never-starved animals. *$P < 0.05$, **$P < 0.01$, and ***$P < 0.001$ (Student's *t*-test).

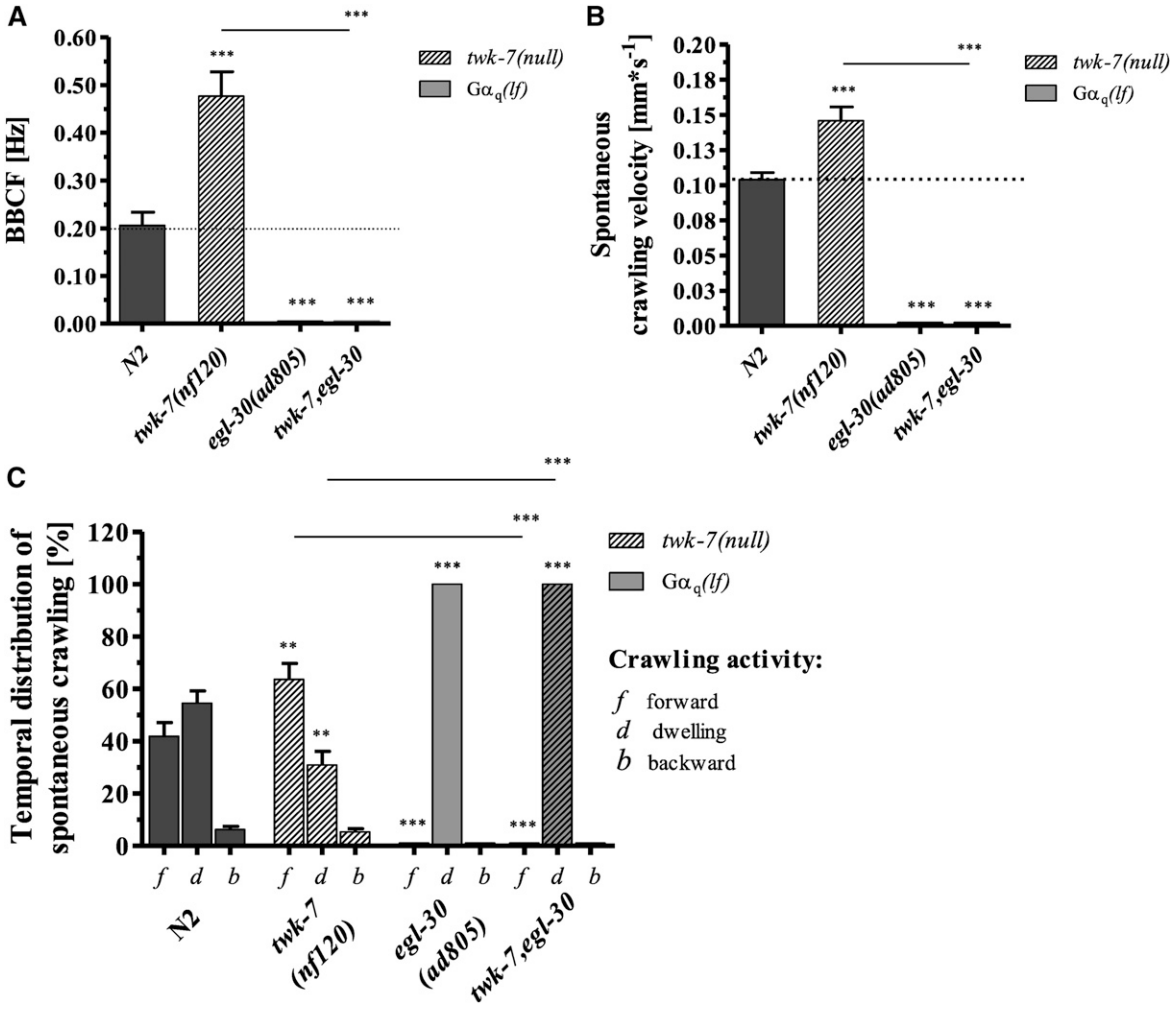

Figure 3 $G\alpha_{q/0}$ signaling is required for the hyperactive phenotype of *twk-7(null)* mutants. (A) The bending frequencies and (B) crawling velocities of single and double mutant animals during spontaneous crawling are shown. (C) The spontaneous locomotion behavior was divided into periods of crawling forward (f), crawling backward (b), and dwelling (d). All values represent the mean (± SEM) of at least $N \geq 3$ independent experiments involving $n \geq 30$ never-starved animals. Dotted lines indicate the wild-type level. $^*P < 0.05$, $^{**}P < 0.01$, and $^{***}P < 0.001$ (Student's *t*-test). BBCF, body-bending crawling frequency.

was reduced by almost 50% in transgenic worms (Figure 4F), and their straightness values dropped from ~80 to 50% (Figure 4G).

Hence, elevated TWK-7 expression specifically in GABAergic motor neurons is sufficient to mitigate the locomotion phenotypes induced by a $G\alpha_S$-KIN-1/PKA(*gf*) genetic background.

Suppression of the $G\alpha_s$ pathway in GABAergic motor neurons does not rescue the hyperactive phenotype of twk-7 (null)

As mentioned above, expression of KIN-2 or dominant negative KIN-2($G^{310}D$) solely in GABAergic D-type motor neurons was sufficient to reverse the hyperactivity and body shape phenotypes of *kin-2(cau1)* mutant worms during spontaneous crawling (Figure 1, B–H). However, in a *twk-7(null)* or *twk-7(null),kin-2(cau1)* background, expression of *kin-2($G^{310}D$)* in GABAergic motor neurons did not change those lines' enhanced velocity and increased BBCF during spontaneous crawling (Figure 4, A and B). In addition, the reduced amplitude-to-body-length ratio during spontaneous and stimulated crawling was not affected (Figure 4, C–E).

Moreover, when *unc-47*p::*kin-2($G^{310}D$)* was introduced in a *twk-7(null)* single or *twk-7(null),kin-2(cau1)* double mutant background, the time spent crawling forward and the straightness of forward crawling during spontaneous locomotion remained unchanged (Figure 4, F and G). Again, the loss of TWK-7 counteracts the inhibitory locomotion effects of an inactive $G\alpha_S$- KIN-1/PKA pathway in GABAergic motor neurons.

In conclusion, an impaired $G\alpha_s$-KIN-1/PKA pathway and the overexpression of TWK-7 in GABAergic motor neurons confer similar lethargic locomotion phenotypes. In both cases, these phenotypes were not affected by an activated KIN-1/PKA background. In contrast, the hyperactivity caused by the loss of TWK-7 completely masked the lethargic locomotion phenotype of GABAergic motor neuron-specific suppression of

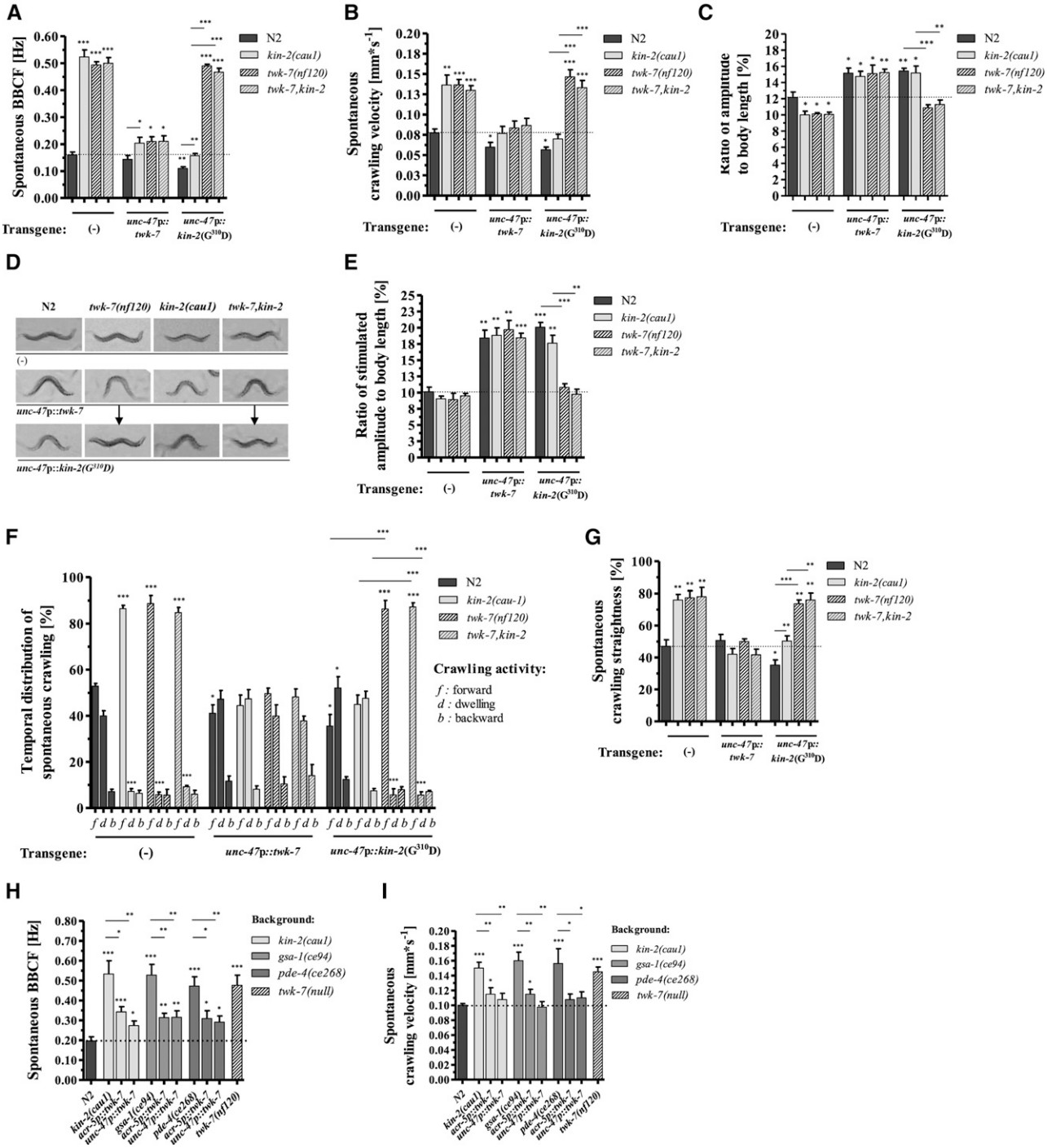

Figure 4 Cell-specific genetic interaction between $G\alpha_S$*(gf)* and *twk-7* in GABAergic motor neurons. (A) The bending frequencies, (B) velocities, and (C) bending-amplitude-to-body-length ratios during spontaneous crawling are shown. (D) Representative pictures of worms during stimulated forward crawling. The arrows indicate the rescue effect on the bending amplitude of worms with a *twk-7(null)* background expressing the KIN-2($G^{310}D$) protein in GABAergic motor neurons. (E) The corresponding amplitude-to-body-length ratios of stimulated animals. Wild-type animals reduced their amplitudes to the level of spontaneously crawling *kin-2(cau1)* and *twk-7(null)* single and double mutants. The amplitudes of these animals were not affected by stimulation. (F) The time that worms spent crawling forward (f), crawling backward (b), or dwelling (d) and (G) the straightness rates during spontaneous crawling are shown. Overexpression of wild-type TWK-7 altered the locomotion phenotypes in all genetic backgrounds. In contrast, the effect of dominant-negative KIN-2($G^{310}D$) expression depends on the genetic background. The locomotion phenotypes of hyperactive *kin-2(cau1)* animals are reversed by the overexpression of KIN-2($G^{310}D$). The locomotion phenotypes of *twk-7(null)* and *twk-7*,*kin-2* double mutants are decisively not affected by KIN-2($G^{310}D$) expression. The (H) spontaneous BBCF and (I) crawling velocities of *kin-2(cau1)*, *gsa-1(ce94)*, and *pde4(ce268)* mutants and the corresponding transgenic worms overexpressing wild-type TWK-7 in cholinergic or GABAergic motor neurons. For comparative reasons, data for N2 wild-types and *twk-7(null)* animals are shown. The effect of GABAergic neuron-specific overexpression of the wild-type form of TWK-7 or of the dominant-negative KIN-2(G310D) protein on locomotor activity and locomotion behavior was investigated in worms with different

the KIN-1/PKA pathway. These results point to a genetic interaction in which TWK-7 is epistatic to KIN-1/PKA, acting downstream to affect multiple aspects of *C. elegans* locomotion including activity, wave shape, and behavior (Figure 5).

Discussion

In this study, we have isolated a novel hyperactivity-related allele of the *C. elegans kin-2* gene, which encodes the negative regulatory subunit of PKA/KIN-1. Detailed analyses revealed that the novel *kin-2(cau1)* allele and other known $G\alpha_S$-PKA *(gf)* mutants (Reynolds *et al.* 2005; Schade *et al.* 2005; Charlie *et al.* 2006) showed a distinct hyperactive locomotion phenotype. Compared to wild-type worms, the phenotype is characterized by fast, straightforward spontaneous locomotion behavior and by spending more time crawling forward at the expense of dwelling periods. In a recent study, we found the same pattern of locomotion phenotypes in mutants that lack the K_2P channel TWK-7 and transgenics that overexpress a dominant negative form of TWK-7 (Lüersen *et al.* 2016). Our genetic interaction studies provide evidence for epistasis between the $G\alpha_s$-KIN-1/PKA pathway and TWK-7 in modulating the locomotor activity and locomotion behavior of *C. elegans* at the level of B- and D-type motor neurons.

The modulation of synaptic transmission by $G\alpha_S$-PKA signaling is a widespread mechanism of neuronal communication. In particular, activation of PKA is known to facilitate transmission by presynaptic mechanisms (Trudeau *et al.* 1996; Nguyen and Woo 2003; Kuromi and Kidokoro 2005; Cheung *et al.* 2006). Several studies in invertebrates and vertebrates have demonstrated that genes involved in cAMP signaling regulate rhythmic physiological processes including locomotor activity and locomotion behavior. Mutations in the *Drosophila* catalytic PKA-C1 subunit and its type II regulatory subunit PKA-RII (homolog of KIN-2) led to behavior-specific arrhythmia and altered spontaneous locomotion behavior (Majercak *et al.* 1997; Park *et al.* 2000). Mice exhibited hyperlocomotor activity when they were deficient in the regulatory subunit RIIβ of PKA (homolog of KIN-2), specifically in the dopamine receptor 2-expressing medium spiny neurons of the striatum, a brain region that regulates motor behaviors (Zheng *et al.* 2013). In mammalian trigeminal motor neurons that participate in rhythmical motor behaviors including suckling, chewing, and swallowing, activation of PKA induced a long-lasting increase in excitability (Bakhshishayan *et al.* 2013). Furthermore, β-adrenergic stimulation of the mammalian heart rate is mediated by PKA, with the L-type Ca^{2+} channel Ca(V)1.2 representing one of the main downstream targets (Hell 2010). Recently, the ability of *C. elegans* KIN-1/PKA to propagate patterned signaling in GABAergic neurons in the context of a rhythmic behavior (namely, the rhythmic defecation cycle) was elucidated in detail. PKA was found to be required in excitatory GABAergic AVL and DVB neurons for the generation of periodic synaptic calcium transients that elicit GABA release and subsequent enteric muscle contraction. The voltage-gated calcium channels (VGCC) UNC-2 (P/Q-type VGCC) and EGL-19 (L-type VGCC) are suggested to function downstream of KIN-1/PKA and promote presynaptic Ca^{2+} influx (Wang and Sieburth 2013). However, in most cases, the downstream targets of PKA that affect rhythmic locomotor output remain elusive.

Our phenotype and genetic interaction studies reveal that $G\alpha_s$-PKA signaling may act in motor neurons upstream of TWK-7 to modulate *C. elegans* locomotor activity and locomotion behavior. In contrast, an activated $G\alpha_S$ pathway did not rescue *twk-7* overexpression in these neurons. Together, these data suggest an epistatic relationship. Unfortunately, employing the same strategy for epistatic analysis in cholinergic B-type motor neurons failed due to dramatic mortality rates, egg-laying defects, and sterility among the isolated transgenic F2 lines carrying an *acr-5p*::*kin-2(G^{310}D)* construct. Consistently, lethality caused by loss of KIN-1/PKA function has been repeatedly reported for *C. elegans* (Kim *et al.* 2012, 2013; Wang and Sieburth 2013; Lee *et al.* 2014). KIN-2 RNA interference produces larval arrest (Schade *et al.* 2005), and animals carrying null mutations in the *kin-1* catalytic and *kin-2* regulatory subunits of PKA die as embryos (van der Linden *et al.* 2008).

Similar to PKA, K_2P channels have been demonstrated to regulate rhythmic processes by modulating the rhythmic presynaptic membrane potential (Lalevee *et al.* 2006; Renigunta *et al.* 2015). Most importantly, some reports have established K_2P channels as downstream targets of the $G\alpha_S$/PKA pathway (Patel *et al.* 1998; Lesage *et al.* 2000; Olschewski *et al.* 2006; Czirjak and Enyedi 2010). PKA activation resulted in the inhibition of the TREK-1 current in mammalian cell culture via phosphorylation at the conserved consensus PKA site Ser^{333} (Patel *et al.* 1998). The K_2P channel TREK-1 is posited to be involved in heart rate regulation (Terrenoire *et al.* 2001). Accordingly, studies on the human cardiac system provide mechanistic evidence to establish cardiac K_2P channels as antiarrhythmic drug targets (Schmidt *et al.* 2012). The activation of TASK-1, a K_2P channel of the human pulmonary artery smooth muscle cells, via PKA phosphorylation might represent an important mechanism underlying vasorelaxation processes (Olschewski *et al.* 2006). Thus, the modulation of the second-messenger cAMP and concurrent PKA activity seems to be read out by certain K_2P channels, resulting in hyperpolarizations and depolarizations, respectively. In this regard, it is notable that an *in silico* analysis of the *C. elegans* TWK-7 amino acid sequence (Neuberger *et al.* 2007) revealed putative KIN-1/PKA

genetic backgrounds [wild-type, *twk-7(null)*, *kin-2(cau1)*, and twk-7(null), *kin-2(cau1)*]. All values in (A and B) and (F–I) represent the mean (± SEM) of at least $N \geq 3$ independent experiments involving $n \geq 30$ never-starved animals. For the measurement of wave parameters in (C) and (E), $N = 3$ independent experiments with $n = 15$ worms per trial were evaluated. $^*P < 0.05$, $^{**}P < 0.01$, and $^{***}P < 0.001$ (Student's *t*-test). Dotted lines indicate the wild-type level. BBCF, body-bending crawling frequency; GABA, γ-aminobutyric acid.

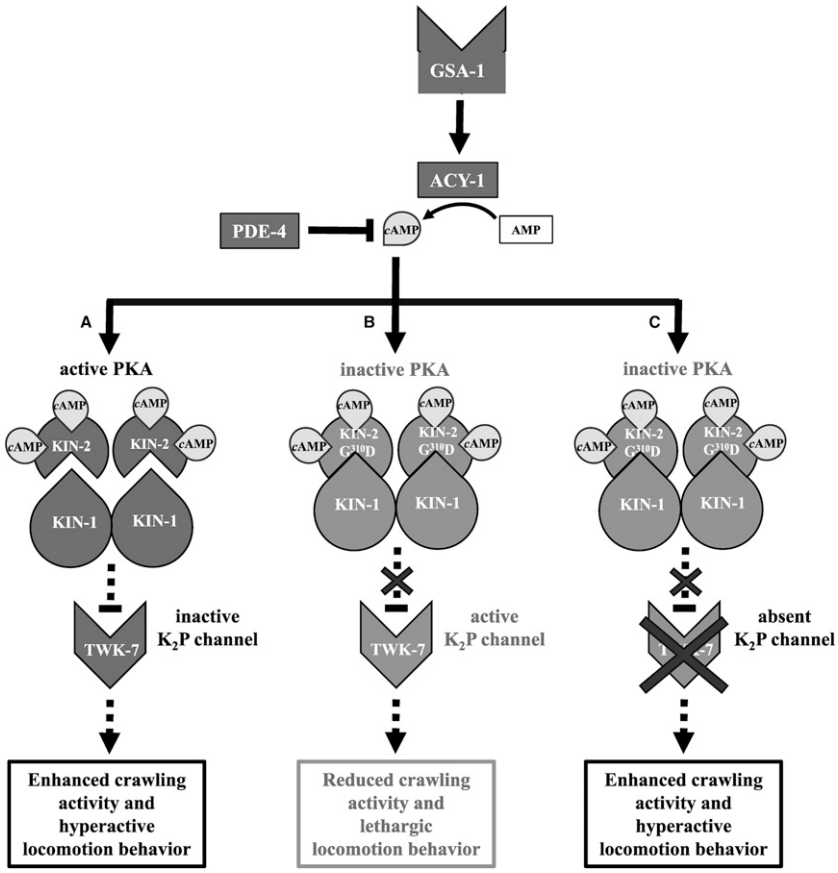

Figure 5 Proposed model of the interplay between the $G\alpha_S$ pathway and the K_2P channel TWK-7 in γ-aminobutyric acid (GABA)ergic motor neurons of *C. elegans*. Stimulation of the G protein-coupled receptor GSA-1 activates the $G\alpha_S$ pathway inducing cAMP synthesis by the adenylate cyclase 1 (ACY-1). Phosphodiesterase 4 (PDE-4) counteracts this process by hydrolyzing cAMP (Reynolds *et al.* 2005; Schade *et al.* 2005). (A) In wild-type background, elevated cAMP levels elicit the dissociation of the two inhibitory KIN-2/RIβ subunits from the KIN-1/KIN-2 heterotetramer causing KIN-1/PKA activation. Accordingly, KIN-1/PKA is hyperactivated in *kin-2* reduction of function mutants such as *kin-2(cau1)* or *kin-2(ce179)* (not depicted in the model). Our data suggest that activated KIN-1/PKA functions epistatically in GABAergic motor neurons to its putative downstream target TWK-7. Inactivation of TWK-7 leads to enhanced locomotor activity and hyperactive locomotion behavior. (B) When overexpressing dominant negative KIN-2($G^{310}D$) in GABAergic motor neurons of wild-type worms, the KIN-1/KIN-2 holoenzyme is insensitive to cAMP and TWK-7 remains active. Therefore, these animals move with reduced crawling activity and exhibit a lethargic locomotion behavior. (C) Acting downstream of KIN-1/PKA, TWK-7(null) rescues the lethargic locomotion phenotype induced by specific overexpression of dominant negative KIN-2($G^{310}D$) in GABAergic motor neurons.

consensus phosphorylation sites at Ser^{81}, Ser^{444}, and Ser^{502} (Figure S1B in File S8). However, epistasis defines a relationship between genes and might not be sufficient to deduce any physical interaction between the resulting proteins (St Onge *et al.* 2007). Moreover, the contribution of different independent pathways that control complex traits (such as locomotion) is often not linear and simply additive but may follow dynamic models, as has been recently demonstrated for the vulval development of *C. elegans* (Corson and Siggia 2012). Accordingly, two pathways (in the case of vulval development, EGF and Notch) that lack any interactive crosstalk showed epistasis due to nonlinear dynamic flow that can be defined by a geometric framework. Therefore, further investigations including phosphorylation assays and site-directed mutation studies are necessary to establish whether there is a physical interaction between KIN-1/PKA and TWK-7 in *C. elegans* motor neurons.

Remarkably, the hyperactive $G\alpha_S$*(gf)* and *twk-7(null)* mutant worms differ significantly in their behavior from hyperactive $G\alpha_{q/0}$ mutants. The respective $G\alpha_q$*(gf)* and $G\alpha_0$*(lf)* mutants with higher DAG levels and elevated acetylcholine release were hyperactive on plates during spontaneous crawling but exhibited decreased swimming activity, spent less time crawling forward, and moved with lower straightness rates. Furthermore, hyperactive *twk-7(null)* and *kin-2(cau1)* mutants are characterized by reduced wave amplitudes during spontaneous crawling. In sharp contrast, hyperactive animals with elevated presynaptic acetylcholine release, such as *egl-30(gf)* and *goa-1(lf)* (Brundage *et al.* 1996; Lackner *et al.* 1999; Huang *et al.* 2008), or increased postsynaptic acetylcholine receptor sensitivity (Bhattacharya *et al.* 2014) moved with enhanced wave amplitudes. Although $G\alpha_q$*(gf)* and $G\alpha_0$*(lf)* animals are characterized by an increased spontaneous body-bending frequency on plates, these worms executed futile back-and-forth movements. Hence, a higher DAG level and concurrent increased acetylcholine output *per se* is apparently not sufficient to promote an acceleration of directed locomotion.

Moreover, our pharmacological assay data suggest that, in contrast to the $G\alpha_{q/0}$ pathway, KIN-1/PKA and TWK-7 affect locomotor activity and locomotion behavior without altering the levels of steady-state acetylcholine release. Similar pharmacological results for $G\alpha_S$*(gf)* mutants have been previously presented (Charlie *et al.* 2006) and have been discussed as being in accordance with electrophysiological data from *Drosophila* $G\alpha_S$*(gf)* mutants (Suzuki *et al.* 2002). Here, the resting spontaneous synaptic current frequency and the nerve-evoked synaptic currents did not differ between wild-type and *dunce* (homolog of PDE) mutant embryos. However, the function of both TWK-7 (shown in this study) and the $G\alpha_S$-PKA pathway (Schade *et al.* 2005) largely depends on $G\alpha_q$, the core vesicle priming pathway, which is a constitutive element for proper locomotion. Hence, we suggest that the $G\alpha_s$-KIN-1/PKA-TWK-7 pathway modulates the locomotor activity of *C. elegans* in the framework of a predetermined $G\alpha_q$-dependent acetylcholine output.

Activation of the $G\alpha_S$-PKA pathway or loss of TWK-7 function (most likely equivalent to a closed TWK-7 channel) influences key parameters of locomotion. Velocity/frequency, amplitude, direction, and persistence are changed in a manner characteristic of coordinated forward movement after specific sensory stimulation (Gaglia and Kenyon 2009; Lüersen *et al.* 2016) or during global food search behavior (Calhoun *et al.* 2014, 2015; Wakabayashi *et al.* 2004). KIN-1/PKA is an established sensor of internal and external cues (Centonze *et al.* 2001; Valjent *et al.* 2005; Yang *et al.* 2014; Goto *et al.* 2015). Therefore, we suggest that an activated $G\alpha_S$-KIN-1/PKA pathway elicits enhanced forward locomotion via suppression of the regulatory K_2P channel TWK-7. This may represent a putative mechanism to promote a complex change in locomotion behavior at the level of motor neurons.

Acknowledgments

We thank D. Sieburth and H. Wang for the wild-type *unc-47p*::*KIN-2* and dominant negative *unc-47p*::*KIN-2(G^{310}D)* genetic constructs. We also thank A. Reinke and F. Neumann for processing plates and strains. Some strains were provided by the *Caenorhabditis* Genetics Center, which is funded by the National Institutes of Health Office of Research Infrastructure Programs (P40 OD-010440). The authors declare that they have no conflicts of interest.

Literature Cited

Aryal, P., F. Abd-Wahab, G. Bucci, M. S. P. Sansom, and S. J. Tucker, 2015 Influence of lipids on the hydrophobic barrier within the pore of the TWIK-1 K2P channel. Channels 9: 44–49.

Bakhshishayan, S., A. Enomoto, T. Tsuji, S. Tanaka, T. Yamanishi *et al.*, 2013 Protein kinase A regulates the long-term potentiation of intrinsic excitability in neonatal trigeminal motoneurons. Brain Res. 1541: 1–8.

Bargmann, C. I., 2012 Beyond the connectome: how neuromodulators shape neural circuits. Bioessays 34: 458–465.

Bhattacharya, R., D. Touroutine, B. Barbagallo, J. Climer, C. M. Lambert *et al.*, 2014 A conserved dopamine-cholecystokinin signaling pathway shapes context-dependent Caenorhabditis elegans behavior. PLoS Genet. 10: e1004584.

Brenner, S., 1974 The genetics of Caenorhabditis elegans. Genetics 77: 71–94.

Brundage, L., L. Avery, A. Katz, U. J. Kim, J. E. Mendel *et al.*, 1996 Mutations in a C. elegans Gqalpha gene disrupt movement, egg laying, and viability. Neuron 16: 999–1009.

Calhoun, A. J., S. H. Chalasani, and T. O. Sharpee, 2014 Maximally informative foraging by Caenorhabditis elegans. Elife 3: e04220.

Calhoun, A. J., A. Tong, N. Pokala, J. A. Fitzpatrick, T. O. Sharpee *et al.*, 2015 Neural mechanisms for evaluating environmental variability in Caenorhabditis elegans. Neuron 86: 428–441.

Centonze, D., B. Picconi, P. Gubellini, G. Bernardi, and P. Calabresi, 2001 Dopaminergic control of synaptic plasticity in the dorsal striatum. Eur. J. Neurosci. 13: 1071–1077.

Chalfie, M., J. E. Sulston, J. G. White, E. Southgate, J. N. Thomson *et al.*, 1985 The neural circuit for touch sensitivity in Caenorhabditis elegans. J. Neurosci. 5: 956–964.

Charlie, N. K., A. M. Thomure, M. A. Schade, and K. G. Miller, 2006 The dunce cAMP phosphodiesterase PDE-4 negatively regulates G alpha(s)-dependent and G alpha(s)-independent cAMP pools in the Caenorhabditis elegans synaptic signaling network. Genetics 173: 111–130.

Cheung, U., H. L. Atwood, and R. S. Zucker, 2006 Presynaptic effectors contributing to cAMP-induced synaptic potentiation in Drosophila. J. Neurobiol. 66: 273–280.

Corson, F., and E. D. Siggia, 2012 Geometry, epistasis, and developmental patterning. Proc. Natl. Acad. Sci. USA 109: 5568–5575.

Czirjak, G., and P. Enyedi, 2010 TRESK background K(+) channel is inhibited by phosphorylation via two distinct pathways. J. Biol. Chem. 285: 14549–14557.

Donnelly, J. L., C. M. Clark, A. M. Leifer, J. K. Pirri, M. Haburcak *et al.*, 2013 Monoaminergic orchestration of motor programs in a complex C. elegans behavior. PLoS Biol. 11: e1001529.

Edwards, M. R., J. R. Johnson, K. Rankin, R. E. Jenkins, C. Maguire *et al.*, 2012 PKC-2 phosphorylation of UNC-18 Ser322 in AFD neurons regulates temperature dependency of locomotion. J. Neurosci. 32: 7042–7051.

Enyedi, P., and G. Czirjak, 2010 Molecular background of leak K+ currents: two-pore domain potassium channels. Physiol. Rev. 90: 559–605.

Fleming, J. T., M. D. Squire, T. M. Barnes, C. Tornoe, K. Matsuda *et al.*, 1997 Caenorhabditis elegans levamisole resistance genes lev-1, unc-29, and unc-38 encode functional nicotinic acetylcholine receptor subunits. J. Neurosci. 17: 5843–5857.

Gaglia, M. M., and C. Kenyon, 2009 Stimulation of movement in a quiescent, hibernation-like form of Caenorhabditis elegans by dopamine signaling. J. Neurosci. 29: 7302–7314.

Gjorgjieva, J., D. Biron, and G. Haspel, 2014 Neurobiology of Caenorhabditis elegans Locomotion: where do we stand? Bioscience 64: 476–486.

Goto, A., I. Nakahara, T. Yamaguchi, Y. Kamioka, K. Sumiyama *et al.*, 2015 Circuit-dependent striatal PKA and ERK signaling underlies rapid behavioral shift in mating reaction of male mice. Proc. Natl. Acad. Sci. USA 112: 6718–6723.

Gray, A. T., B. B. Zhao, C. H. Kindler, B. D. Winegar, M. J. Mazurek *et al.*, 2000 Volatile anesthetics activate the human tandem pore domain baseline K+ channel KCNK5. Anesthesiology 92: 1722–1730.

Gray, J., and H. W. Lissmann, 1964 The Locomotion of nematodes. J. Exp. Biol. 41: 135–154.

Grillner, S., 2006 Biological pattern generation: the cellular and computational logic of networks in motion. Neuron 52: 751–766.

Hell, J. W., 2010 Beta-adrenergic regulation of the L-type Ca2+ channel Ca(V)1.2 by PKA rekindles excitement. Sci. Signal. 3: pe33.

Hu, S., T. Pawson, and R. M. Steven, 2011 UNC-73/trio RhoGEF-2 activity modulates Caenorhabditis elegans motility through changes in neurotransmitter signaling upstream of the GSA-1/Galphas pathway. Genetics 189: 137–151.

Huang, K. M., P. Cosman, and W. R. Schafer, 2008 Automated detection and analysis of foraging behavior in Caenorhabditis elegans. J. Neurosci. Methods 171: 153–164.

Jorgensen, E. M., and S. E. Mango, 2002 The art and design of genetic screens: Caenorhabditis elegans. Nat. Rev. Genet. 3: 356–369.

Kiehn, O., 2006 Locomotor circuits in the mammalian spinal cord. Annu. Rev. Neurosci. 29: 279–306.

Kim, S., J. A. Govindan, Z. J. Tu, and D. Greenstein, 2012 SACY-1 DEAD-Box helicase links the somatic control of oocyte meiotic maturation to the sperm-to-oocyte switch and gamete maintenance in Caenorhabditis elegans. Genetics 192: 905–928.

Kim, S., C. Spike, and D. Greenstein, 2013 Control of oocyte growth and meiotic maturation in Caenorhabditis elegans. Adv. Exp. Med. Biol. 757: 277–320.

Kuromi, H., and Y. Kidokoro, 2005 Exocytosis and endocytosis of synaptic vesicles and functional roles of vesicle pools: lessons from the Drosophila neuromuscular junction. Neuroscientist 11: 138–147.

Lackner, M. R., S. J. Nurrish, and J. M. Kaplan, 1999 Facilitation of synaptic transmission by EGL-30 Gqalpha and EGL-8 PLCbeta: DAG binding to UNC-13 is required to stimulate acetylcholine release. Neuron 24: 335–346.

Lalevee, N., B. Monier, S. Senatore, L. Perrin, and M. Semeriva, 2006 Control of cardiac rhythm by ORK1, a Drosophila two-pore domain potassium channel. Curr. Biol. 16: 1502–1508.

Larkman, P. M., and E. M. Perkins, 2005 A TASK-like pH- and amine-sensitive 'leak' K+ conductance regulates neonatal rat facial motoneuron excitability in vitro. Eur. J. Neurosci. 21: 679–691.

Lee, J. H., J. Kong, J. Y. Jang, J. S. Han, Y. Ji *et al.*, 2014 Lipid droplet protein LID-1 mediates ATGL-1-dependent lipolysis during fasting in Caenorhabditis elegans. Mol. Cell. Biol. 34: 4165–4176.

Lesage, F., C. Terrenoire, G. Romey, and M. Lazdunski, 2000 Human TREK2, a 2P domain mechano-sensitive K+ channel with multiple regulations by polyunsaturated fatty acids, lysophospholipids, and Gs, Gi, and Gq protein-coupled receptors. J. Biol. Chem. 275: 28398–28405.

Lüersen, K., U. Faust, D. C. Gottschling, and F. Doring, 2014 Gait-specific adaptation of locomotor activity in response to dietary restriction in Caenorhabditis elegans. J. Exp. Biol. 217: 2480–2488.

Lüersen, K., D. C. Gottschling, and F. Doring, 2016 Complex locomotion behavior changes are induced in Caenorhabditis elegans by the lack of the regulatory leak K+ channel TWK-7. Genetics 204: 683–701.

Ma, D. K., M. Rothe, S. Zheng, N. Bhatla, C. L. Pender *et al.*, 2013 Cytochrome P450 drives a HIF-regulated behavioral response to reoxygenation by C. elegans. Science 341: 554–558.

Mahoney, T. R., S. Luo, and M. L. Nonet, 2006 Analysis of synaptic transmission in Caenorhabditis elegans using an aldicarb-sensitivity assay. Nat. Protoc. 1: 1772–1777.

Majercak, J., D. Kalderon, and I. Edery, 1997 Drosophila melanogaster deficient in protein kinase A manifests behavior-specific arrhythmia but normal clock function. Mol. Cell. Biol. 17: 5915–5922.

Marder, E., D. Bucher, D. J. Schulz, and A. L. Taylor, 2005 Invertebrate central pattern generation moves along. Curr. Biol. 15: R685–R699.

Marder, E., M. L. Goeritz, and A. G. Otopalik, 2014 Robust circuit rhythms in small circuits arise from variable circuit components and mechanisms. Curr. Opin. Neurobiol. 31C: 156–163.

McIntire, S. L., E. Jorgensen, and H. R. Horvitz, 1993 Genes required for GABA function in Caenorhabditis elegans. Nature 364: 334–337.

McKay, S. J., R. Johnsen, J. Khattra, J. Asano, D. L. Baillie *et al.*, 2003 Gene expression profiling of cells, tissues, and developmental stages of the nematode C. elegans. Cold Spring Harb. Symp. Quant. Biol. 68: 159–169.

Miller, K. G., M. D. Emerson, and J. B. Rand, 1999 Goalpha and diacylglycerol kinase negatively regulate the Gqalpha pathway in C. elegans. Neuron 24: 323–333.

Minevich, G., D. S. Park, D. Blankenberg, R. J. Poole, and O. Hobert, 2012 CloudMap: a cloud-based pipeline for analysis of mutant genome sequences. Genetics 192: 1249–1269.

Neuberger, G., G. Schneider, and F. Eisenhaber, 2007 pkaPS: prediction of protein kinase A phosphorylation sites with the simplified kinase-substrate binding model. Biol. Direct 2: 1.

Nguyen, P. V., and N. H. Woo, 2003 Regulation of hippocampal synaptic plasticity by cyclic AMP-dependent protein kinases. Prog. Neurobiol. 71: 401–437.

Nurrish, S., L. Segalat, and J. M. Kaplan, 1999 Serotonin inhibition of synaptic transmission: Galpha(0) decreases the abundance of UNC-13 at release sites. Neuron 24: 231–242.

Olschewski, A., Y. Li, B. Tang, J. Hanze, B. Eul *et al.*, 2006 Impact of TASK-1 in human pulmonary artery smooth muscle cells. Circ. Res. 98: 1072–1080.

Park, S. K., S. A. Sedore, C. Cronmiller, and J. Hirsh, 2000 Type II cAMP-dependent protein kinase-deficient Drosophila are viable but show developmental, circadian, and drug response phenotypes. J. Biol. Chem. 275: 20588–20596.

Patel, A. J., and E. Honore, 2001 Anesthetic-sensitive 2P domain K+ channels. Anesthesiology 95: 1013–1021.

Patel, A. J., E. Honore, F. Maingret, F. Lesage, M. Fink *et al.*, 1998 A mammalian two pore domain mechano-gated S-like K+ channel. EMBO J. 17: 4283–4290.

Perrier, J. F., A. Alaburda, and J. Hounsgaard, 2003 5–HT1A receptors increase excitability of spinal motoneurons by inhibiting a TASK-1-like K+ current in the adult turtle. J. Physiol. 548: 485–492.

Renigunta, V., G. Schlichthorl, and J. Daut, 2015 Much more than a leak: structure and function of K-2P-channels. Pflugers Arch. 467: 867–894.

Reynolds, N. K., M. A. Schade, and K. G. Miller, 2005 Convergent, RIC-8-dependent Galpha signaling pathways in the Caenorhabditis elegans synaptic signaling network. Genetics 169: 651–670.

Sawin, E. R., R. Ranganathan, and H. R. Horvitz, 2000 C. elegans locomotory rate is modulated by the environment through a dopaminergic pathway and by experience through a serotonergic pathway. Neuron 26: 619–631.

Schade, M. A., N. K. Reynolds, C. M. Dollins, and K. G. Miller, 2005 Mutations that rescue the paralysis of Caenorhabditis elegans ric-8 (synembryn) mutants activate the G alpha(s) pathway and define a third major branch of the synaptic signaling network. Genetics 169: 631–649.

Schmidt, C., F. Wiedmann, P. A. Schweizer, R. Becker, H. A. Katus *et al.*, 2012 Novel electrophysiological properties of dronedarone: inhibition of human cardiac two-pore-domain potassium (K2P) channels. Naunyn Schmiedebergs Arch. Pharmacol. 385: 1003–1016.

Sieburth, D., J. M. Madison, and J. M. Kaplan, 2007 PKC-1 regulates secretion of neuropeptides. Nat. Neurosci. 10: 49–57.

St Onge, R. P., R. Mani, J. Oh, M. Proctor, E. Fung *et al.*, 2007 Systematic pathway analysis using high-resolution fitness profiling of combinatorial gene deletions. Nat. Genet. 39: 199–206.

Suzuki, K., A. D. Grinnell, and Y. Kidokoro, 2002 Hypertonicity-induced transmitter release at Drosophila neuromuscular junctions

is partly mediated by integrins and cAMP/protein kinase A. J. Physiol. 538: 103–119.
Terrenoire, C., I. Lauritzen, F. Lesage, G. Romey, and M. Lazdunski, 2001 A TREK-1-like potassium channel in atrial cells inhibited by beta-adrenergic stimulation and activated by volatile anesthetics. Circ. Res. 89: 336–342.
Trudeau, L. E., D. G. Emery, and P. G. Haydon, 1996 Direct modulation of the secretory machinery underlies PKA-dependent synaptic facilitation in hippocampal neurons. Neuron 17: 789–797.
Valjent, E., V. Pascoli, P. Svenningsson, S. Paul, H. Enslen *et al.*, 2005 Regulation of a protein phosphatase cascade allows convergent dopamine and glutamate signals to activate ERK in the striatum. Proc. Natl. Acad. Sci. USA 102: 491–496.
van der Linden, A. M., S. Wiener, Y. J. You, K. Kim, L. Avery *et al.*, 2008 The EGL-4 PKG acts with KIN-29 salt-inducible kinase and protein kinase A to regulate chemoreceptor gene expression and sensory behaviors in Caenorhabditis elegans. Genetics 180: 1475–1491.
Vidal-Gadea, A., S. Topper, L. Young, A. Crisp, L. Kressin *et al.*, 2011 Caenorhabditis elegans selects distinct crawling and swimming gaits via dopamine and serotonin. Proc. Natl. Acad. Sci. USA 108: 17504–17509.
Wakabayashi, T., I. Kitagawa, and R. Shingai, 2004 Neurons regulating the duration of forward locomotion in Caenorhabditis elegans. Neurosci. Res. 50: 103–111.
Wang, H., and D. Sieburth, 2013 PKA controls calcium influx into motor neurons during a rhythmic behavior. PLoS Genet. 9: e1003831.
Wen, Q., M. D. Po, E. Hulme, S. Chen, X. Liu *et al.*, 2012 Proprioceptive coupling within motor neurons drives C. elegans forward locomotion. Neuron 76: 750–761.
White, J. G., E. Southgate, J. N. Thomson, and S. Brenner, 1976 The structure of the ventral nerve cord of Caenorhabditis elegans. Philos. Trans. R. Soc. Lond. B Biol. Sci. 275: 327–348.
Wilm, T., P. Demel, H. U. Koop, H. Schnabel, and R. Schnabel, 1999 Ballistic transformation of Caenorhabditis elegans. Gene 229: 31–35.
Yang, L., M. L. Gilbert, R. Zheng, and G. S. McKnight, 2014 Selective expression of a dominant-negative type Ialpha PKA regulatory subunit in striatal medium spiny neurons impairs gene expression and leads to reduced feeding and locomotor activity. J. Neurosci. 34: 4896–4904.
Yost, C. S., 2000 Tandem pore domain K channels: an important site of volatile anesthetic action? Curr. Drug Targets 1: 207–217.
Yu, H., B. Aleman-Meza, S. Gharib, M. K. Labocha, C. J. Cronin *et al.*, 2013 Systematic profiling of Caenorhabditis elegans locomotive behaviors reveals additional components in G-protein Galphaq signaling. Proc. Natl. Acad. Sci. USA 110: 11940–11945.
Zhang, J., M. Cao, X. Wu, Y. Chen, W. Liang *et al.*, 2015 Enhanced expression of TWIK-related arachidonic acid-activated K+ channel in the spinal cord of detrusor overactivity rats after partial bladder outlet obstruction. BMC Urol. 15: 100.
Zheng, R. M., L. H. Yang, M. A. Sikorski, L. C. Enns, T. A. Czyzyk *et al.*, 2013 Deficiency of the RII beta subunit of PKA affects locomotor activity and energy homeostasis in distinct neuronal populations. Proc. Natl. Acad. Sci. USA 110: E1631–E1640.
Zhou, K. M., Y. M. Dong, Q. Ge, D. Zhu, W. Zhou *et al.*, 2007 PKA activation bypasses the requirement for UNC-31 in the docking of dense core vesicles from C. elegans neurons. Neuron 56: 657–669.

Communicating editor: P. Sengupta